INTERNATIONAL JOURNAL OF CLIMATOLOGY
Int. J. Climatol. **34**: 2678–2684 (2014)
Published online 6 November 2013 in Wiley Online Library
(wileyonlinelibrary.com) DOI: 10.1002/joc.3867

RMetS
Royal Meteorological Society

Drought and wetness variability in the Tarim River Basin and connection to large-scale atmospheric circulation

Hui Tao,[a]* Hartmut Borth,[b] Klaus Fraedrich,[b] Buda Su[c] and Xiuhua Zhu[b]

[a] *State Key Laboratory of Lake Science and Environment, Chinese Academy of Sciences, Nanjing Institute of Geography and Limnology, Nanjing, China*

[b] *KlimaCampus, Universität Hamburg, Hamburg, Germany*

[c] *National Climate Center, China Meteorological Administration, Beijing, China*

ABSTRACT: On the basis of daily observations of 39 meteorological stations in the Tarim River Basin, the variability of drought and wetness has been analysed using the standardized precipitation-evapotranspiration index (SPEI, 1961–2010). The result shows an increasing trend in annual mean SPEI with a significant change in 1986. Although the frequency of moderate and severe droughts decreased after the change, the frequency of extreme drought events increased slightly. But different categories of wetness show a consistent increase in frequency. The return periods of drought and wetness prolonged and shortened, respectively, after 1986. Furthermore, composites of geopotential height and water vapour flux fields at 500 hPa are analyzed for extreme wet and dry months of the warm season (May to October) as well as for the warm seasons of the periods 1961 to 1986 and 1987 to 2010. The difference between composites of extreme wet and dry shows that the water vapour supply during wet events can be related to transports from the Arabian Sea and the Bay of Bengal. The midlatitude atmospheric circulation plays an important role by transporting moisture from the east into the Tarim River Basin; this is the main reason of the wetter condition in warm seasons after 1986 in the study region.

KEY WORDS drought and wetness variability; Tarim River Basin; large-scale circulation

Received 12 June 2013; Revised 4 October 2013; Accepted 11 October 2013

1. Introduction

Drought and wetness fluctuations have profound effects on ecosystems, hydrology and agriculture, especially for arid and semi-arid regions of central Asia. As a drought-prone region, consequent feedbacks of drought and wetness in this area control the availability of water across the landscape and influence the distribution of vegetation and the dominant agricultural model (Aizen *et al.*, 2001; Piao *et al.*, 2010; Vicente-Serrano *et al.*, 2013). Numerous studies have been documented drought and wetness variability in large parts of the planet and on the possible physical causes of these phenomena by employing different drought indices. The most broadly used indices include the Palmer drought severity index (PDSI) (Dai *et al.*, 2004, Sheffield and Wood, 2008) and the standardized precipitation index (SPI) (McKee *et al.*, 1993; Bordi *et al.*, 2006, 2009; Bothe *et al.*, 2010; Zhu *et al.*, 2010; Sienz *et al.*, 2012). However, the SPI is based only on precipitation data, and does not consider other critical variables such as evapotranspiration, which can have a marked influence on drought conditions. The simplicity of the PDSI, which is calculated from a simple water-balance model forced by monthly precipitation and temperature data, makes it an attractive tool in large-scale drought assessments, but may give biased results in the context of climate change (Sheffield *et al.*, 2012). This implies that more realistic calculations, based on the underlying physical principles, should be taken into account. Furthermore, lacks of the multiscalar character makes the PDSI not a reliable index for identifying different drought types. For those reasons, a new drought index [standardized precipitation-evapotranspiration index (SPEI)] based on precipitation and potential evapotranspiration (PET) was proposed by Vicente-Serrano *et al.* (2010), which combines the physical principles of the PDSI with the multiscalar character of the SPI.

In northwest China, it was widely believed that a phase of warm and dry conditions ended in 1980s and changed to warm and increasingly humid conditions, especially in the Tarim River Basin, which has been characterized as a consequence of global warming and an intensified water cycle (Shi *et al.*, 2006; Chen *et al.*, 2008; Xu *et al.*, 2010). By using monthly gridded precipitation from the Climatic Research Unit (CRU), Chen *et al.* (2011) concluded that the variations of westerly circulation are likely the major factors that influence the precipitation variations in the Central Asia. Bothe *et al.* (2012) also argue that moisture supply to these areas is primarily due to the mid-latitude westerlies with contributions

* Correspondence to: H. Tao, State Key Laboratory of Lake Science and Environment, Chinese Academy of Sciences, Nanjing Institute of Geography and Limnology, Nanjing 210008, China. E–mail: htao@niglas.ac.cn

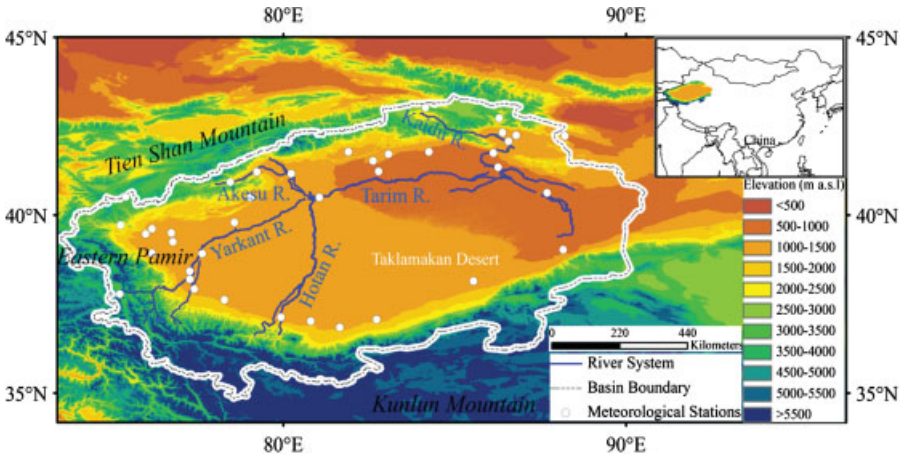

Figure 1. Geographical location and topographic map of the Tarim River Basin.

from higher latitudes. To better interpret these changes, more work is needed to understand drought and wetness variability in the Tarim River Basin and the causes of the recent fluctuations, which could be beneficial in many ways for this area. Obviously, these studies are also important for understanding the climate change in the arid regions of western China. However, in China, most of the related studies have focused on the eastern monsoon region (Bothe *et al.*, 2010; Zhang *et al.*, 2009; Gemmer *et al.*, 2011), while drought and wetness in the Tarim River Basin and the possible association with large-scale atmospheric circulation are rarely studied.

In light of the significance of precipitation in arid regions, it is important to understand temporal variability of drought and wetness over the Tarim River Basin and to reveal their relationship with large-scale atmospheric circulation patterns. The objective of this paper is (1) to detect temporal variability of drought and wetness and (2) to explore possible causes behind drought and wetness variations in the Tarim River Basin during the warm season.

2. Climatological setting, methodology and data

2.1. Climatological setting

The Tarim River Basin is located in the northwest of China. It covers an area of 102×10^4 km^2 (Figure 1, 35°–43°N,74°–90°E). The Tarim River, which is one of the world's largest closed continental rivers, originates from the surrounding mountains, meanders through the northern border of the central flat desert (Taklamakan desert) without outflow (Tao *et al.*, 2008). The four source rivers (Akesu, Hotan, Yarkant and Kaidu River) discharge into the Tarim River Basin mainly depends on the onset of the dry or wet period and on their extension in time and space in the headstream region.

High mountains with orographically enhanced precipitation like Tien Shan, Eastern Pamir, Kunlun and Karakorum mountains surround the Tarim River Basin and act as barriers; that is, water vapour transports by the Indian Monsoon from the southwest and by the Southeast Monsoon from the Pacific Ocean are blocked. The main factor determining the climatic regimes of the Tarim River Basin is the interaction between the southwestern branch of the Siberian anticyclonic circulation and cyclonic activity from the west (Aizen *et al.*, 1997). The steep gradients of elevation and high interannual variability of precipitation make the hydrologic and climatic feedbacks in the Tarim River Basin different from those in lower-elevation or humid regions in China and other regions in the world. The multiannual means of precipitation range from about 30 mm in the central flat desert up to 270 mm in the highest mountainous areas surrounding the Tarim River Basin. Precipitation in the mountain areas surrounding the basin can exceed 300 mm per year in some areas and it is mostly in the form of snowfall. The precipitation annual cycle of the entire basin is characterized by rainfall maxima during May to August (Bothe *et al.*, 2012).

2.2. Standardized precipitation-evapotranspiration index (SPEI)

SPEI has been introduced by Vicente-Serrano *et al.* (2010). The estimation is based on the difference between monthly mean precipitation and PET based on the Penman-Monteith equation (recommended by Food and Agriculture Organization of the United Nations (FAO), Allen *et al.*, 1998). More detailed information on the calculation of the SPEI can be found in the Appendix. The subsequent SPEI-classification provides cumulative probabilities of drought and wetness occurrences as listed in Table 1.

To investigate the temporal variability of drought and wetness, a combination of cumulative sum charts (CUSUM) and bootstrapping methods (suggested by Taylor, 2000) were applied to the annual average SPEI time series for the period 1961–2010. The significance of the monthly SPEI trend at each station is analysed by the commonly used Mann–Kendall's (MK) test (Kahya and Kalayci, 2004). The return period of drought and

Table 1. SPEI classification and corresponding cumulative probabilities of occurrence.

Category	SPEI value	Cumulative probability (%)
Extremely wet	SPEI ≥ 2	2.28
Moderately wet	$1.5 \leq$ SPEI < 1.99	6.68
Slightly wet	$1 \leq$ SPEI < 1.49	15.87
Near normal	$-0.99 <$ SPEI < 0.99	50.00
Mild drought	$-1.49 <$ SPEI ≤ -1	84.13
Moderate drought	$-1.99 <$ SPEI ≤ -1.5	93.32
Extreme drought	SPEI ≤ -2	97.72

wetness is calculated as follows: first, the mean (μ) and standard deviation (σ) of monthly SPEI are obtained by the normal distribution function, and then the probability density function (P) at each of the values in SPEI is calculated using the normal distribution with μ and σ. This finally provides the return period $T = 1/P$ (The WAFO Group, 2000). The analysis of the relationship between drought/wetness and the large-scale atmospheric circulation is based on the monthly mean geopotential height and water vapour flux fields at 500 hPa.

2.3. Data

Daily precipitation, temperature, wind speed, relative humidity, sunshine duration and water vapour pressure datasets of 39 meteorological stations over the Tarim River Basin (Figure 1) are provided by the Climate Center of Xinjiang Province (1961–2010). The original datasets have been tested for inhomogeneities using the standard normal homogeneity test (SNHT) developed by Alexandersson and Moberg (1997). As the results do not reveal any inhomogeneity points, the original series is used. For analysis of the large-scale atmospheric circulation, monthly mean geopotential height and water vapour flux fields ($2.5^\circ \times 2.5^\circ$) at 500 hPa are taken from the National Center for Environmental Prediction/National Center for Atmospheric Research (NCEP-NCAR) reanalysis data for the time period 1961–2010.

3. Temporal variability of SPEI

Before we investigate the possible cause of the drought and wetness variations in the Tarim River Basin, it is important to have an appreciation of the temporal variability of the SPEI. Figure 2(a) shows the linear fit indicating an increasing trend of the annual average SPEI in the Tarim River Basin. Significant change points can be found in 1986, consistent with change points documented for precipitation, relative humidity, vapour pressure and an aridity index of the Tarim River Basin (Tao *et al.*, 2011). The spatial distribution of linear trends in annual SPEI for each station is shown in Figure 2(b), and increasingly wet conditions were observed over the north of the basin during the period 1961–2010, while negative trends were only observed in few stations. The increasing wet conditions (SPEI ≥ 1) are also identified by the SPEI at different timescales, with minor short-term droughts presented after 1986 (Figure 2(c)). However,

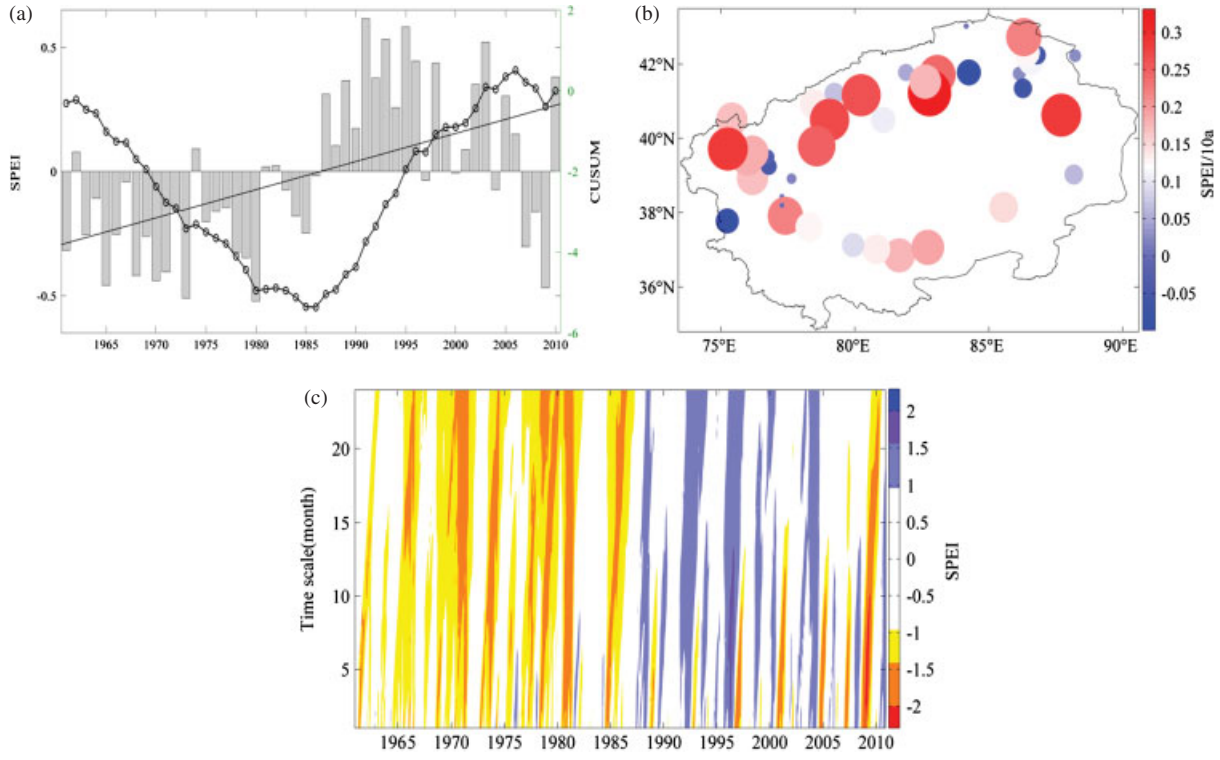

Figure 2. Temporal (a) (straight and dot lines denote linear trend and cumulative sum, respectively) and spatial (b) variability of annual SPEI based on linear trend test and (c) SPEI at different timescale (1 to 24 months) for the period 1961–2010 in the Tarim River Basin.

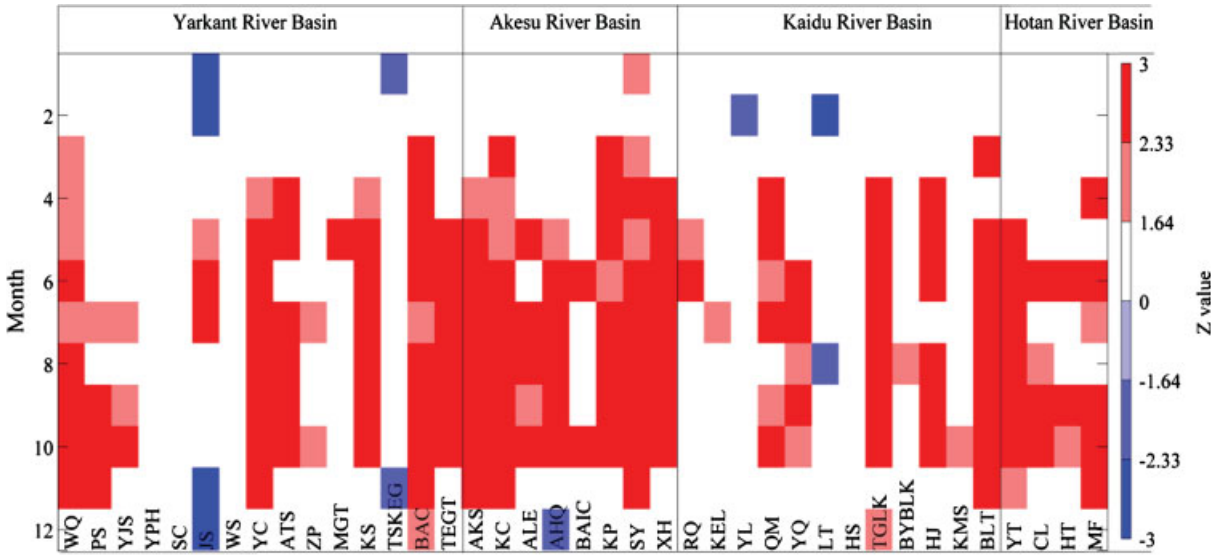

Figure 3. MK trend test of monthly SPEI from 1961 to 2010; stations and months with increase (decrease) of trends significant on 95% confidence level in red (blue); non-significant trends are left in white; the x-axis denotes the stations.

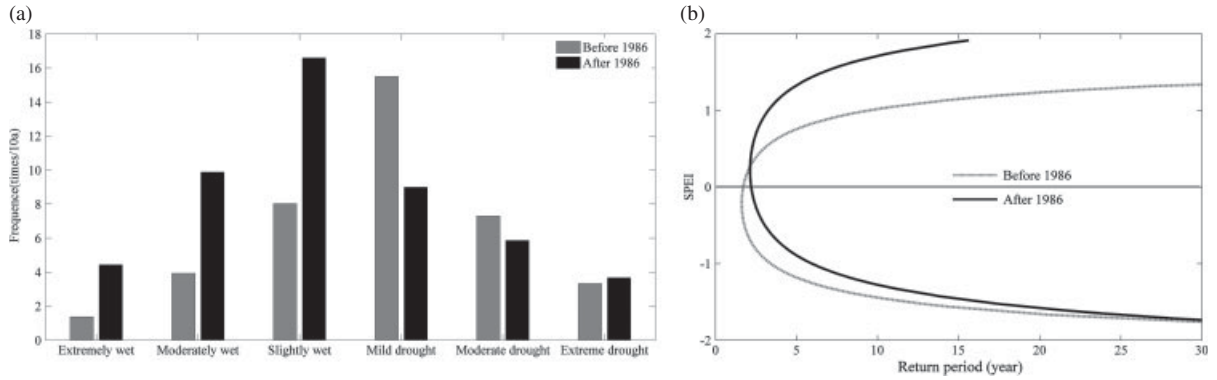

Figure 4. Changes of frequency (a) and return period (b) of drought and wetness before and after 1986.

a long-term drought (SPEI ≤ -1) also occurred during 2008–2009.

For a detailed investigation, the monthly SPEI trend (1961–2010) is also analysed for each station employing the MK trend test. It is found that stations show (Figure 3) significantly increasing trends predominantly in warm seasons (May to October), only few stations show significant trends in cold season (November to April). In warm seasons, more significant increasing trends can be found in the stations located in Akesu River Basin; this is also in agreement with the streamflow trends of the Akesu River Basin reported by Tao *et al.* (2011).

The frequency of occurrence for each drought and wetness category of all stations (expressed as times per 10 years) is shown in Figure 4(a) (left vertical axis) for the periods 1961–1986 and 1987–2010. It appears that in all wetness categories the frequency has almost doubled, while a decrease in frequency can be found in mild and moderate drought during the period 1987–2010. The frequency of drought and wetness can also be expressed by the associated return period; for illustrative purposes, Figure 4(b) presents the return period plots of different drought and wetness categories for 1961–1986 and 1987–2010. As expected, the return periods of most wetness categories have shortened after 1986. Conversely, the return periods of all drought categories have prolonged, which is consistent with the decreased frequency of occurrence in mild to moderate drought after 1986. Moreover, intensified wet conditions also can be concluded from the shape of the return period curve after 1986, while the dry conditions alleviated a little.

4. Large-scale atmospheric circulation: a possible link

The 1986 change point of annual average SPEI identified by the CUSUM method is associated with significantly increasing trends in warm seasons. In order to better understand the possible drivers of drought and wetness variability, we focus on synchronous changes in large-scale circulation patterns employing composite analysis of geopotential height and water vapour flux anomalies at 500 hPa for extreme wet

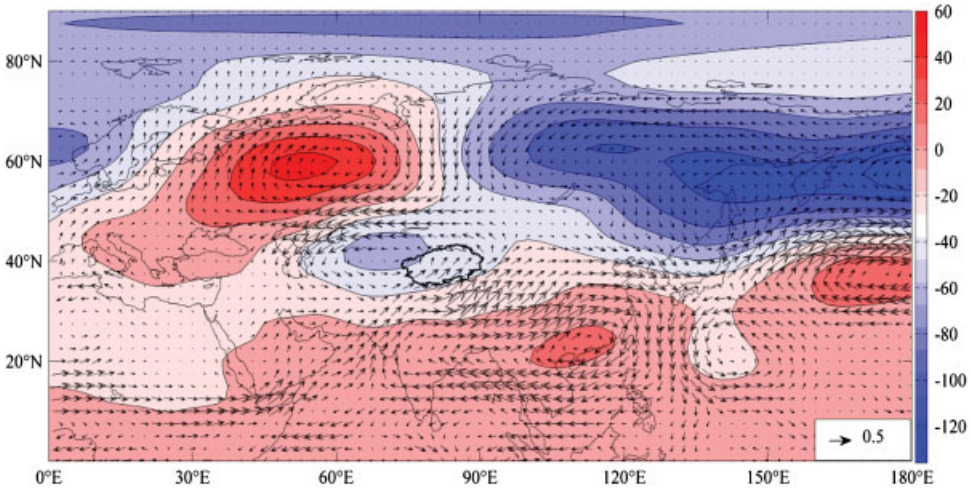

Figure 5. Water vapour flux (unit: kg m^{-1} s^{-1}) and geopotential height anomalies (unit: gpm) at 500 hPa for extreme wet and dry months of the warm season (MJJASO, 1961–2010: wet month minus dry month).

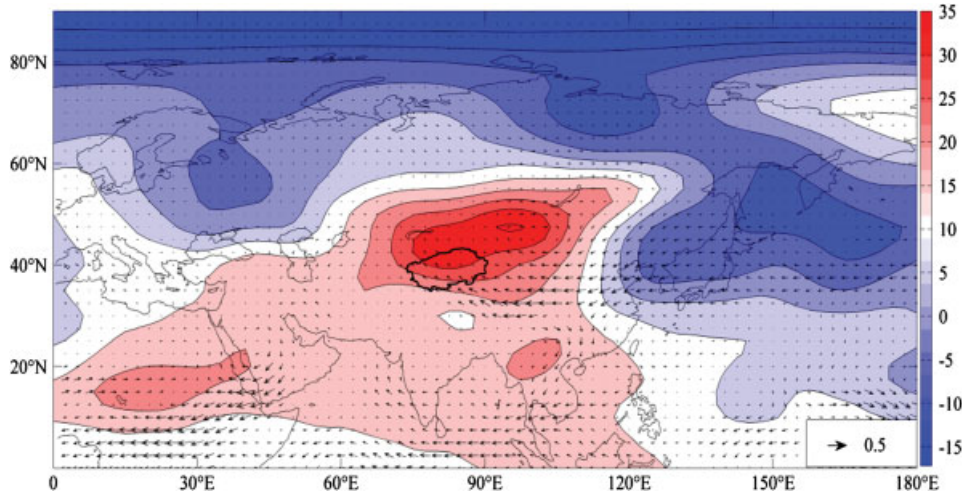

Figure 6. Water vapour flux (unit: kg m^{-1} s^{-1}) and geopotential height anomalies (unit: gpm) at 500 hPa in the warm season periods (after minus before 1986).

(more than 50% of the stations with SPEI > 2) and extreme dry month (more than 50% stations with SPEI < -2) during the warm seasons from May to October for the period 1961–2010 (Figure 5); meanwhile, water vapour flux and geopotential height anomalies between 1961–1986 and 1987–2010 were also composited for warm seasons. The following results are noted:

1. The water vapour flux anomalies of the extreme wet minus the extreme dry month composites (six cases, respectively) reveal two main steering centres, which determine the atmospheric water transport branches over the Tarim River Basin: (a) An intense anticyclone (positive geopotential height anomaly) centred over northern Europe enhances the westward transport of water vapour. (b) A southwesterly circulation anomaly transports water vapour from the Arabian Sea and the Bay of Bengal into the Tarim River Basin in extreme wet months. (c) The composition of water vapour flux fields of extreme wet and dry months does not rule out a connection to the monsoonal circulation.
2. Warm season composites of water vapour flux and geopotential height anomalies (500 hPa) for 1961–1986 and 1987–2010, respectively, show humid conditions increasing since 1986 as documented by the water flux and geopotential height differences (Figure 6). That is, the western North Pacific subtropical high (with positive height anomalies) extending over the Mongolian plateau and negative height anomalies in the higher latitudes (poleward of 60°N) lead to an increase of the water vapour transport from the east. The northeasterly wind in northern and eastern China has strengthened, and went in parallel with a weakening of the northern extent of the westerly jet stream.

5. Summary and discussion

The present analysis identifies 1986 as a significant turning point of the annually averaged standardized precipitation-evaporation index, SPEI, characterizing drought and wetness of the Tarim River Basin. A significantly increasing trend of the SPEI occurs at most stations in the warm season, which implies that wetter conditions since 1986 may be related to an intensified global hydrological cycle. This is consistent with the statistics of frequency of droughts (decreasing) and wetness (increasing) at almost all stations of the basin. As a result, the return period of drought and wetness categories have prolonged and shortened, respectively, after 1986. There is general consensus that northwest China benefits from an integrated circulation that combines with the southwest flow, Arctic Ocean's cold flow and westerly circulation, leading to a gradual increase in wetness (Dai *et al.*, 2007; Xu *et al.*, 2010; Bothe *et al.*, 2012). In this study, the relation of drought and wetness with large-scale circulation patterns shows that origins of water vapour supply related to wet extreme months are different from those related to dry extreme month. Wet extreme months are connected to an increased moisture transport from the Arabian Sea and the Bay of Bengal. The midlatitude atmospheric circulation plays an important role by transporting moisture from the east into the Tarim River Basin; this is the main reason of the wetter condition in warm seasons after 1986 in the study region. The results of the current study shed light on the changing features of the drought and wetness and the underlying causes, which will be greatly helpful for better understanding of the hydro-climatic changes in the Tarim River Basin.

On the basis of a global climate model, the role of black carbon on precipitation was studied by Menon *et al.* (2002), who emphasized the increasing trend in precipitation over northern China being caused by aerosol forcing; Rosenfeld *et al.* (2008) also argue that the effect of an increased concentration of sub-cloud aerosol, and hence cloud condensation nuclei (CCN), on convective clouds is to invigorate updrafts and produce more precipitation. So, we can deduce that the increasingly humid conditions after 1986 are probably due to the increasing ocean–land thermal difference caused by an increased aerosol optical depth during the warm season over East China, leading to a further northward extension of the summer monsoon into North China.

Acknowledgements

This study was supported by the German Science Foundation [DFG, Climate change and water resources in western China (Aksu-Tarim), PAK 393], the National Basic Research Program of China (No. 2012CB955903) and the National Natural Science Foundation of China (No. 41101023). Thanks also extend to the German Academic Exchange Service (DAAD) and the Max Planck Fellowship (KF).

Appendix

Standardized precipitation-evapotranspiration index (SPEI)

The standardized precipitation-evapotranspiration index (SPEI) is estimated on a monthly basis as follows: (1) Firstly potential evapotranspiration (PET) is derived by the Penman-Monteith equation recommended by FAO (Allen *et al.*, 1998). With a given value of PET, the difference D between precipitation P and PET for the month 'i' is calculated by

$$D_i = P_i - \mathrm{PET}_i \tag{A1}$$

Step 2 involves the accumulation of D_i calculated above at different timescales and a normalization of D_i into a log-logistic probability distribution to obtain the SPEI series. The probability density function of a three parameter log-logistic distribution is expressed as

$$F(x) = \frac{\beta}{\alpha} \quad \frac{(x-\gamma)^{\beta-1}}{\alpha} \left[1 + \frac{(x-\gamma)^{\beta}}{\alpha}\right]^{-2} \tag{A2}$$

where α, β and γ are scale, shape and origin parameters, respectively, which can be obtained by the L-moment method:

$$\alpha = \frac{(w_0 - 2w_1)\,\beta}{\Gamma(1+1/\beta)\,\Gamma(1-1/\beta)} \tag{A3}$$

$$\beta = \frac{2w_1 - w_0}{6w_1 - w_0 - 6w_2} \tag{A4}$$

$$\gamma = w_0 - \alpha\Gamma(1+1/\beta)\,\Gamma(1-1/\beta) \tag{A5}$$

where $\Gamma(\beta)$ is the gamma function of β. The probability-weighted moments of the original D_i time series are calculated as

$$w_s = \frac{1}{N}\sum_{i=1}^{N}(1-F_i)^s\,D_i \tag{A6}$$

$$F_i = \frac{i - 0.35}{N} \tag{A7}$$

where N is the number of data points. On the basis of formula (A3), the SPEI can be calculated as follows:

$$\text{When } P \le 0.5,\ P = 1 - F(x) \tag{A8}$$

$$w = \sqrt{-2\ln(P)} \tag{A9}$$

$$\mathrm{SPEI} = w - \frac{c_0 + c_1 w + c_2 w^2}{1 + d_1 w + d_2 w^2 + d_3 w^3} \tag{A10}$$

where, the constants are $c_0 = 2.515517$, $c_1 = 0.802853$, $c_2 = 0.010328$, $d_1 = 1.432788$, $d_2 = 0.189269$ and $d_3 = 0.001308$. If $P > 0.5$, then P is replaced by

$1 - P$ and the sign of the resulting SPEI is reversed (Vicente-Serrano *et al.*, 2010).

References

Aizen VB, Aizen EM, Melack JM, Dozier J. 1997. Climatic and hydrologic changes in the Tien Shan, Central Asia. *J. Climate* **10**: 1393–1404.

Aizen EM, Aizen VB, Melack JM, Nakamura T, Ohta T. 2001. Precipitation and atmospheric circulation patterns at mid-latitudes of Asia. *Int. J. Climatol.* **21**: 535–556.

Alexandersson H, Moberg A. 1997. Homogenization of Swedish temperature data. Part I: homogeneity test for linear trends. *Int. J. Climatol.* **17**: 25–34.

Allen RG, Pereira LS, Raes D. 1998. Crop evapotranspiration guidelines for computing crop water requirements. FAO Irrigation and Drainage Paper No.56 FAO. Rome.

Bordi I, Fraedrich K, Petitta M, Sutera A. 2006. Large-scale assessment of drought variability based on NCEP/NCAR and ERA-40 reanalyses. *Water Resour. Manag.* **20**: 899–915.

Bordi I, Fraedrich K, Sutera A. 2009. Observed drought and wetness trends in Europe: an update. *Hydrol. Earth Syst. Sci.* **13**: 1519–1530.

Bothe O, Fraedrich K, Zhu XH. 2010. The large-scale circulations and summer drought and wetness on the Tibetan plateau. *Int. J. Climatol.* **30**: 844–855.

Bothe O, Fraedrich K, Zhu XH. 2012. Precipitation climate of Central Asia and the large-scale atmospheric circulation. *Theor. Appl. Climatol.* **108**: 345–354.

Chen X, Wu JL, Hu Q. 2008. Simulation of climate change impacts on streamflow in the Bosten Lake basin using an artificial Neural Network Model. *J. Hydrol. Eng.* **13**: 180–183.

Chen FH, Huang W, Jin LY, Chen JH, Wang JS. 2011. Spatiotemporal precipitation variations in the arid Central Asia in the context of global warming. *Sci. China Earth Sci.* **54**(12): 1812–1821.

Dai AG, Trenberth KE, Qian TT. 2004. A global dataset of Palmer drought severity index for 1870–2002: relationship with soil moisture and effects of surface warming. *J. Hydrometeorol.* **5**: 1117–1130.

Dai XG, Li WJ, Ma ZG, Wang P. 2007. Water-vapor source shift of Xinjiang region during the recent twenty years. *Proc. Natl. Acad. Sci. U. S. A.* **17**(5): 569–575.

Gemmer M, Fischer T, Jiang T, Su BD, Liu LL. 2011. Trends in precipitation extremes in the Zhujiang river basin, South China. *J. Climate* **24**: 750–761.

Kahya E, Kalayci S. 2004. Trend analysis of streamflow in Turkey. *J. Hydrol.* **289**: 128–144.

McKee TB, Doesken NJ, Kleist J. 1993. The relationship of drought frequency and duration to time scales. In *Proceedings of the 8th Conference on Applied Climatology*, Anaheim, CA, 179–184.

Menon S, Hansen J, Nazarenko L, Luo YF. 2002. Climate effects of black carbon aerosols in China and India. *Science* **297**: 2250–2253.

Piao SL, Ciais P, Huang Y, Shen ZH, Peng SS, Li JS, Zhou LP, Liu HY, Ma YC, Ding YH, Friedlingstein P, Liu CZ, Tan K, Yu YQ, Zhang TY, Fang JY. 2010. The impacts of climate change on water resource and agriculture in China. *Nature* **467**: 43–51.

Rosenfeld D, Lohmann U, Raga GB, O'Dowd CD, Kulmala M, Fuzzi S, Reissell A, Andreae MO. 2008. Flood or drought: how do aerosols affect precipitation? *Science* **321**: 1309–1313.

Sheffield J, Wood EF. 2008. Global Trends and variability in soil moisture and drought characteristics, 1950–2000, from observation-driven simulations of the terrestrial hydrologic cycle. *J. Climate* **21**: 432–457.

Sheffield J, Wood EF, Roderick ML. 2012. Little change in global drought over the past 60 years. *Nature* **491**: 435–438, DOI: 10.1038/nature11575.

Shi YF, Shen YP, Kang ES, Li DL, Ding YJ, Zhang GW, Hu RJ. 2006. Recent and future climate change in northwest China. *Clim. Change* **80**(3–4): 379–393, DOI: 10.1007/s10584-006-9121-7.

Sienz F, Bothe O, Fraedrich K. 2012. Monitoring and quantifying future climate projections of dryness and wetness extremes: SPI bias. *Hydrol. Earth Syst. Sci.* **8**: 10635–10677.

Tao H, Gemmer M, Song YD, Jiang T. 2008. Eco-hydrological responses on water division in the lower reaches of the Tarim River, China. *Water Resour. Res.* **44**: W08422, DOI: 10.1029/2007wr006186.

Tao H, Gemmer M, Bai YG, Su BD, Mao WY. 2011. Trends of streamflow in the Tarim River Basin during the past fifty years: human impact or climate change? *J. Hydrol.* **400**: 1–9.

Taylor WA. 2000. Change-Point Analysis: A Powerful New Tool for Detecting Changes. http://www.variation.com/cpa/tech/changepoint.html.

The WAFO Group. 2000. WAFO–Tutorial. Mathematical Statistics, Centre for Mathematical Sciences, Lund University.

Vicente-Serrano SM, Beguería S, López-Moreno JI. 2010. A multiscalar drought index sensitive to global warming: the standardized precipitation evapotranspiration index. *J. Climate* **23**: 1696–1718.

Vicente-Serrano SM, Gouveia C, Camarero JJ, Beguería S, Trigo R, López-Moreno JI, Azorín-Molina C, Pasho E, Lorenzo-Lacruz J, Revuelto J, Morán-Tejeda E, Sanchez-Lorenzo A. 2013. Response of vegetation to drought time-scales across global land biomes. *Proc. Natl. Acad. Sci. U. S. A.* **110**(1): 52–57.

Xu LG, Zhou HF, Liang C, Du L, Li H. 2010. Spatial and temporal variability of annual and seasonal precipitation over the desert region of China during 1951–2005. *Hydrol. Process.* **24**: 2947–2959.

Zhang ZX, Tao H, Zhang Q, Zhang JC, Forther N, Hoermann G. 2009. Moisture budget variations in the Yangtze River Basin, China, and possible associations with large-scale circulation. *Stoch. Environ. Res. Risk Assess.* **24**: 579–589.

Zhu X, Bothe O, Fraedrich K. 2010. Summer atmospheric bridging between Europe and East Asia: influences on drought and wetness on the Tibetan Plateau. *Quater. Int.* **236**(1–2): 151–157.

